

Cosmography from well-localized Fast Radio Bursts

Jéferson A. S. Fortunato,^{1*} Wiliam S. Hipólito-Ricaldi,^{1,2} Marcelo V. dos Santos^{3,4,5,6}

¹PPGCosmo, CCE, Universidade Federal do Espírito Santo (UFES), Av. Fernando Ferrari, 540, CEP 29.075-910, Vitória, ES, Brazil

²Núcleo Cosmo-UFES & Departamento de Ciências Naturais, CEUNES, Universidade Federal do Espírito Santo (UFES), Rodovia BR 101 Norte, km. 60, CEP 29.932-540, São Mateus, ES, Brazil

³Fundação Coppetec, Rua Moniz de Aragão, 360 - Bloco 1 - Cidade Universitária da Universidade Federal do Rio de Janeiro (UFRJ), CEP 21941-594, Rio de Janeiro, RJ, Brazil

⁴Núcleo de Pesquisa Aplicada à Meios Geológicos-Geotécnicos, Av. Athos da Silveira Ramos, 149 - Bloco I, 203 - Cidade Universitária da Universidade Federal do Rio de Janeiro (UFRJ), Rio de Janeiro - RJ, 21941-909

⁵Instituto de Física, Universidade de São Paulo (USP), R. do Matão, 1371 - Butantã, 05508-09 - São Paulo, SP, Brazil

⁶Unidade Acadêmica de Física, Universidade Federal de Campina Grande (UFCG), R. Aprígio Veloso, Bodocongó, 58429-900 - Campina Grande, PB, Brazil

Accepted XXX. Received YYY; in original form ZZZ

ABSTRACT

Fast Radio Bursts (FRBs) are millisecond-duration pulses occurring at cosmological distances that have emerged as prominent cosmological probes due to their dispersion measure (DM) evolution with redshift. In this work, we use cosmography, a model-independent approach to describe the evolution of the universe, to introduce the cosmographic expansion of the DM-z relation. By fitting two different models for the intergalactic medium and host contributions to a sample of 23 well-localized FRBs, we estimate the kinematic parameters $q_0 = -0.59_{-0.17}^{+0.20}$, $j_0 = 1.08_{-0.56}^{+0.62}$, $s_0 = -2.1 \pm 7.0$, and $H_0 = 69.4 \pm 4.7$ achieving a precision of 6% and 7% for the Hubble constant depending on the models used for contributions. Furthermore, we demonstrate that this approach can be used as an alternative and complementary cosmological-model independent method to revisit the long-standing "Missing Baryons" problem in astrophysics by estimating that 82% of the baryonic content of the universe resides in the intergalactic medium, within 7% and 8% precision, according to the contribution models considered here. Our findings highlight the potential of FRBs as a valuable tool in cosmological research and underscore the importance of ongoing efforts to improve our understanding of these enigmatic events.

Key words: Fast radio bursts – Cosmography – Intergalactic medium

1 INTRODUCTION

Fast Radio Bursts (FRBs) are a class of extremely bright and short-duration transients that occur in the radio spectrum and last for only a few milliseconds. They exhibit large dispersion measures (DMs), which are a measure of the electron column density along the sight-line. The observed DMs significantly exceed the contribution expected from the Milky Way, providing strong evidence for their extragalactic origin (Lorimer et al. 2007; Petroff et al. 2019). Since the first FRB discovery in 2007 by Duncan Lorimer and his team, hundreds of bursts have been reported, and some of these FRBs are known to be repeaters (Zhou et al. 2022). Among these bursts, 24 have been precisely localised, and their host galaxy and redshift have been determined. While some FRB events have been linked to magnetars (Bochenek et al. 2020), numerous progenitor models have been proposed in the literature (Zhang 2020; Bhandari et al. 2020). The cosmological origin of these FRBs has made them a prominent observable in the study of cosmology.

The so-called "Hubble tension" is a discrepancy between two different methods of estimating the expansion rate of the Universe, known as the Hubble constant (H_0). One way of estimating the Hubble constant involves observations of the cosmic microwave back-

ground (CMB) radiation, which is a relic of the early universe. The Planck Collaboration (Aghanim et al. 2020) utilised this technique and obtained a value of $H_0 = 67.4 \pm 0.5 \text{ km s}^{-1} \text{ Mpc}^{-1}$. Another approach is to measure the distances and parallax using cepheid stars and type Ia supernovae in the local universe to infer H_0 directly. This method was employed by Riess et al. (2022) who found a significantly higher value of $H_0 = 73.04 \pm 1.04 \text{ km s}^{-1} \text{ Mpc}^{-1}$, differing by 5σ from the previous method. In this context, it is important to identify alternative observables that can verify the tension. Fast Radio Bursts have already been used as a tool to infer H_0 (Macquart et al. 2020; Wu et al. 2022; Zhao et al. 2022; Hagstotz et al. 2022). However, additional data is required to increase the accuracy of the measurement and determine which value is preferred.

Another cosmological issue that can be addressed by the use of FRBs is the "missing baryons problem". According to measurements obtained by the Planck Collaboration (Aghanim et al. 2020), the CMB radiation suggests that the vast majority of the Universe, $\sim 95\%$, is comprised of dark energy and dark matter, with only a small fraction, approximately 5%, of baryonic matter. However, in the low-redshift universe has been noted a baryon deficit (Fukugita et al. 1998). This deficit could arise from a not complete understanding of the baryons distribution in the universe and thus, it is important to study the baryon budget. Through a series of observations, Shull et al. (2012) suggested that, at low-redshift, roughly 18% of the baryon budget can

* E-mail: jeferson.fortunato@edu.ufes.br

be accounted for by stars, galaxies, circumgalactic medium (CGM), intracluster medium (ICM), and cold neutral gas, while the remaining 82% exists in a diffuse state within the intergalactic medium (IGM), that is, a fraction of baryons in IGM of $f_{\text{IGM}} \approx 0.82$. To cite a few results in literature: using five localised FRBs, [Li et al. \(2020\)](#) estimated a value of $f_{\text{IGM}} = 0.84^{+0.16}_{-0.22}$. The authors in [\(Lemos et al. 2022\)](#), through a model-independent technique and using a sample of 17 FRBs with redshift measurement found $f_{\text{IGM}} = 0.881 \pm 0.012$. In [\(Yang et al. 2022\)](#), the authors obtained $f_{\text{IGM}} = 0.83 \pm 0.06$ using 22 localised FRBs.

Additionally, FRBs have emerged as a potentially powerful tool for investigating a broad range of applications in astrophysics and fundamental physics. These include the detection of the baryon content in the universe ([McQuinn 2014; Deng & Zhang 2014](#)), constraints in equation of state for dark energy ([Zhou et al. 2014; Gao et al. 2014](#)), trace the magnetic fields in the intergalactic medium ([Akahori et al. 2016](#)), test the equivalence principle ([Wei et al. 2015; Tingay & Kaplan 2016; Nusser 2016](#)), and constraint the rest mass of photons ([Wu et al. 2016; Shao & Zhang 2017; Lin et al. 2023](#)), among others. Regarding H_0 and f_{IGM} constraints, it must be stressed that most of the cases mentioned above were performed for a particular cosmological model: the Λ CDM. However, we would get a complementary perspective if any model-independent method were used.

One of the most noticeable model-independent approaches in cosmology is the cosmography. This method, which has been extensively discussed in previous works ([Weinberg 1972; Visser 2005; Aviles et al. 2012](#)), relies solely on the cosmological principle and employs the FLRW metric. Unlike other approaches that require the use of Friedmann equations derived from General Relativity, the cosmography expands observable quantities such as luminosity distance into power series and establishes a direct relationship between cosmological parameters and the available data. This approach has been extensively utilised in prior research employing a range of cosmological probes including Baryon Acoustic Oscillations, Type Ia supernovae, and Cosmic Chronometers ([Lazkoz et al. 2013; Riess et al. 2022; Jalilvand & Mehrabi 2022](#)). However, it has not yet been applied to Fast Radio Bursts.

Fast Radio Bursts dispersion measure (DM) has been suggested as a possible and complementary tool to other established techniques in cosmology. It is interesting to explore the application of cosmographic expansion to the DM and examine the insights that FRBs can offer regarding the cosmographic approach. The present paper applies cosmography to the FRBs dispersion measure-redshift ($\text{DM} - z$) relationship to determine some cosmographic parameters (deceleration parameter q_0 , jerk parameter j_0 and snap parameter s_0), including the Hubble constant using the most recent set of well-localised FRBs. Furthermore, we estimate the fraction of baryons present in the intergalactic medium (IGM). The paper is structured as follows: In Section 2, we discuss the fundamental properties of FRBs. In Section 3, we introduce the cosmographic equations. Section 4 outlines methods for the likelihood computation. We present our data and results in Section 5, and finally, we discuss the results in Section 6.

2 PROPERTIES OF FRBS

During its path to earth, a FRB pulse is dispersed by the intergalactic medium. The amount of dispersion is given by the time delay of different radio frequencies that compose the signal observed:

$$\Delta t \propto \left(\nu_{\text{lo}}^{-2} - \nu_{\text{hi}}^{-2} \right) \text{DM}, \quad (1)$$

where ν_{lo} and ν_{hi} represents the low and high frequencies respectively. The dispersion measure DM is related to the column density of free electrons n_e along the FRB line of sight l weighted by redshift as

$$\text{DM} = \int \frac{n_e}{(1+z)} dl. \quad (2)$$

The observed DM_{obs} includes two main contributions from the intergalactic and extra-galactic mediums, DM_{local} and DM_{EG} :

$$\text{DM}_{\text{obs}} = \text{DM}_{\text{local}} + \text{DM}_{\text{EG}}(z), \quad (3)$$

being

$$\text{DM}_{\text{local}} = \text{DM}_{\text{ISM}} + \text{DM}_{\text{halo}}, \quad (4)$$

and

$$\text{DM}_{\text{EG}} = \text{DM}_{\text{IGM}} + \frac{\text{DM}_{\text{host}}}{(1+z)}, \quad (5)$$

where DM_{ISM} corresponds to the contributions from the Milky Way interstellar medium, usually calculated through galactic electron distribution models such as NE2001 ([Cordes & Lazio 2002](#)) and YMW16 ([Yao et al. 2017](#)) then subtracted from the observed DM. Here we used NE2001 approach because in recent works it has been reported that YMW16 model may overestimate DM_{ISM} at low Galactic latitudes ([Ocker et al. 2021](#)). On the other hand, DM_{halo} is related to Milk Way galactic halo which has been estimated in the range of $50 < \text{DM}_{\text{halo}} < 100 \text{ pc cm}^{-3}$ ([Prochaska & Zheng 2019](#)). However, to be conservative we assume $\text{DM}_{\text{halo}} = 50 \text{ pc cm}^{-3}$ as for example in [\(Macquart et al. 2020\)](#). DM_{IGM} is the contribution from the intergalactic medium (IGM) which has cosmological dependence and DM_{host} is the host galaxy component corrected with $(1+z)^{-1}$ to account for cosmological expansion for a FRB source at redshift z .

The dominant contribution to the observed dispersion measure of a FRB signal is due to the intergalactic medium (IGM). In a previous study, [McQuinn \(2013\)](#) reported that this component is responsible for an expressive scatter around the mean DM_{IGM} , $100 - 400 \text{ pc cm}^{-3}$ at $z = 0.5 - 1$, respectively. Following [Deng & Zhang \(2014\)](#), the average DM_{IGM} is given by

$$\langle \text{DM}_{\text{IGM}} \rangle = A \Omega_b H_0 \int_0^z \frac{(1+z') f_{\text{IGM}}(z') f_e(z')}{E(z')} dz', \quad (6)$$

where $E(z) = H(z)/H_0$, $f_e = Y_{\text{H}} X_{e,\text{H}}(z) + \frac{1}{2} Y_{\text{He}} X_{e,\text{He}}(z)$ and $A = 3c/8\pi G m_p$. The cosmic baryon density, the mass of proton and the fraction of baryon mass in the IGM are represented by Ω_b , m_p and f_{IGM} , respectively. In this work we also consider an IGM with a hydrogen mass fraction $Y_{\text{H}} = 0.75$ and a helium mass fraction $Y_{\text{He}} = 0.25$. Given the fact that hydrogen and helium are completely ionized at $z < 3$, the ionization fractions of each species are $X_{e,\text{H}} = X_{e,\text{He}} = 1$. For this analysis, first, we keep a constant value for the fraction of baryon mass, $f_{\text{IGM}} = 0.82$ ([Shull et al. 2012](#)) but after we leave it as a free parameter.

According to equation (3), DM_{IGM} is estimated by $\text{DM}_{\text{IGM}} = \text{DM}_{\text{obs}} - \text{DM}_{\text{local}} - \text{DM}_{\text{host}}(1+z)^{-1}$ with uncertainty given as

$$\sigma_{\text{IGM}}(z) = \sqrt{\sigma_{\text{obs}}(z)^2 + \sigma_{\text{local}}^2 + \left(\frac{\sigma_{\text{host}}(z)}{1+z} \right)^2}, \quad (7)$$

where σ_{obs} and σ_{host} are the errors related to DM_{obs} and DM_{host} , respectively. Whereas σ_{local} is the sum of DM_{ISM} and DM_{halo} uncertainties, we follow [Hagstotz et al. \(2022\)](#) taking $\sigma_{\text{local}} \approx 30 \text{ pc/cm}^{-3}$.

The scatter around the averaged quantity $\langle \text{DM}_{\text{IGM}} \rangle$ is due to inhomogeneities in the column density of free electrons along the FRB

line of sight. The distribution of DM_{IGM} is greatly influenced by the way how baryons are distributed around galactic halos as shown by cosmological simulations. The number of collapsed structures that a given line of sight intersects, it determines the extent of variation around $\langle DM_{\text{IGM}} \rangle$ thus, more compact halos leads to a skewed probability distribution associated with $\langle DM_{\text{IGM}} \rangle$, while a more diffuse gas around the halos results in a more Gaussian-like probability distribution function (Macquart et al. 2015, 2020; Bhandari & Flynn 2021). In the literature, both approaches have been studied. For example in (Prochaska et al. 2019a; Yang et al. 2022; Wu et al. 2020), non-gaussian approach was used, while in (Jaroszynski 2019; Hagstotz et al. 2022; Zhang et al. 2023), considered the gaussian point of view. In this work, we use these two approaches to model the IGM component looking forward to detect any possible different impact on final conclusions.

The first approach we use is more conservative as it assumes a gaussian distribution around the mean, given by equation (6), with standard deviation interpolated in the range $\sigma_{\text{IGM}}(z=0) \approx 10 \text{ pc cm}^{-3}$ and $\sigma_{\text{IGM}}(z=1) \approx 400 \text{ pc cm}^{-3}$. This method was used, for instance, in Hagstotz et al. (2022). In the second approach, we follow Macquart et al. (2020) and assume a quasi-gaussian distribution for the IGM contribution:

$$P_{\text{IGM}}(\Delta) = A\Delta^{-\beta} \exp\left[-\frac{(\Delta^{-\alpha} - C_0)}{2\alpha^2\sigma_{\text{DM}}^2}\right], \quad \Delta > 0, \quad (8)$$

being $\Delta \equiv DM_{\text{IGM}}/\langle DM_{\text{IGM}} \rangle$. This approach, which has shown excellent agreement with the observed distributions of DM_{IGM} in both semi-analytic models and hydrodynamic simulations, is based on the fact that when the variance σ_{DM} is large, it captures the skewness due to the different sightlines that cross a few large structures increasing the DM_{IGM} value. Conversely, in the limit of small σ_{DM} , the distribution of Eq. (8) becomes Gaussian. The parameters α and β are related to the inner density profile of gas inside galactic halos. We use the values from Macquart et al. (2020), $\alpha = 3$ and $\beta = 3$. The remaining two parameters A and C_0 are fitted when $\Delta = 1$. The standard deviation with redshift of DM_{IGM} can be estimated by

$$\sigma_{\text{DM}} = Fz^{-0.5}, \quad (9)$$

where F quantifies how strong is the baryon feedback, that is, how diffuse is the gas around the halo. Following Macquart et al. (2020), we assume $F = 0.32$.

Although the dispersion measure of the host environment DM_{host} is a crucial feature to determine the source, it still has few theoretical motivations. In order to estimate this component, informations about the host galaxy type, electron distribution, position of FRB signal within the galaxy, and the viewing angle are required. However, all of these information are still uncertain and thus we focus on the probability distribution of DM_{host} . Here we consider two cases for modeling the DM_{host} : the first one, following Hagstotz et al. (2022), it is based on the stochastic contribution:

$$P(DM_{\text{host}}) = \mathcal{N}(\langle DM_{\text{host}} \rangle, \sigma_{\text{host}}^2), \quad (10)$$

being \mathcal{N} a normal distribution. For this approach, we assume galactic halos similar to the Milky Way, then for the mean value we have $\langle DM_{\text{host}} \rangle = 100(1 + z_{\text{host}})^{-1} \text{ pc cm}^{-3}$ and for the variance, $\sigma_{\text{host}} = 50(1 + z_{\text{host}})^{-1} \text{ pc cm}^{-3}$.

The second case, we follow Macquart et al. (2020) and consider a log-normal distribution, as it has a long asymmetric tail allowing for large DM_{host} values:

$$P(DM_{\text{host}}) = \frac{1}{DM_{\text{host}}\sigma_{\text{host}}\sqrt{2\pi}} \exp\left(-\frac{\ln DM_{\text{host}} - \mu}{2\sigma_{\text{host}}^2}\right), \quad (11)$$

where e^μ and $e^{2\mu + \sigma_{\text{host}}^2}(e^{\sigma_{\text{host}}^2} - 1)$ are the mean and variance of the distribution, respectively.

3 COSMOGRAPHY WITH FAST RADIO BURSTS

Cosmography, or cosmic kinematics, plays an important role when studying cosmic expansion in a model-independent way, i.e., without dependence on any specific model for the underlying cosmic evolution. This approach is based on the cosmological principle, which postulates the homogeneity and isotropy of the Universe on large scales. In order to describe the kinematics of the cosmic expansion, one needs to use the Hubble parameter:

$$H(t) = \frac{1}{a} \frac{da}{dt}, \quad (12)$$

and additionally the functions (Visser 2005),

$$q(t) = -\frac{1}{a} \frac{d^2a}{dt^2} \left(\frac{1}{a} \frac{da}{dt}\right)^{-2}, \quad (13)$$

$$j(t) = \frac{1}{a} \frac{d^3a}{dt^3} \left(\frac{1}{a} \frac{da}{dt}\right)^{-3}, \quad (14)$$

and

$$s(t) = -\frac{1}{a} \frac{d^4a}{dt^4} \left(\frac{1}{a} \frac{da}{dt}\right)^{-4}. \quad (15)$$

The cosmological expansion rate is characterized by $H(t)$, while the deceleration parameter, $q(t)$, represents the acceleration or deceleration of the universe's expansion. The jerk parameter $j(t)$ can be used to estimate if there was a transition period in which the universe modified its expansion by changing the rate of the expansion acceleration. Additionally, the snap parameter, $s(t)$, is important to discriminate between a cosmological model that allows an evolving dark energy term or one with a cosmological constant. Although there exists also other parameters that includes higher-order time derivatives of the scale factor, we focus only in $H(t)$, $q(t)$, $j(t)$ and $s(t)$.

By using the parameters defined above, scale factor can be expanded around the present time, t_0 as

$$\begin{aligned} \frac{a(t)}{a_0} &= 1 + H_0(t - t_0) - \frac{1}{2}q_0H_0^2(t - t_0)^2 \\ &+ \frac{1}{3!}j_0H_0^3(t - t_0)^3 + \frac{1}{4!}s_0H_0^4(t - t_0)^4 + O\left[(t - t_0)^5\right]. \end{aligned} \quad (16)$$

From now on, we set $a_0 = 1$ and H_0 , q_0 , j_0 and s_0 stand for the quantities evaluated in current time t_0 . Eq. (16) helps us to find the cosmographic series for $E(z)$ -function, with which it is possible to obtain the expansion for luminosity distance, angular distance, redshift drift (see for example Lobo et al. (2020); Heinesen (2021); Pourojaghi et al. (2022); Rocha & Martins (2023)) or in our case, the $DM_{\text{IGM}}(z)$ given by eq.(6). To do this we use the relation:

$$\frac{dH}{dz} = \left(\frac{1+q}{1+z}\right)H, \quad (17)$$

and obtain the DM – z relation in terms of cosmographic parameters,

$$\begin{aligned} \text{DM}_{\text{IGM}}(z) &= \frac{3\Omega_b H_0^2}{8\pi G m_p} f_e f_{\text{IGM}} \left\{ \frac{cz}{H_0} \left[1 - \frac{q_0 z}{2} \right. \right. \\ &+ \frac{1}{6} (4 + 6q_0 + 3q_0^3 - j_0) z^2 \\ &- \frac{1}{24} (18q_0 + 42q_0^2 + 14q_0 j_0 - 9q_0^3 - s_0 - 18j_0) z^3 \\ &\left. \left. + O(z^4) \right\}. \end{aligned} \quad (18)$$

The Taylor series, as shown in eq.(18), exhibits convergence issues for high-redshifts ($z > 1$). This concern prompted [Cattoën & Visser \(2007\)](#) to address the convergence problems and propose a new parametrization, denoted as $y = z(1+z)^{-1}$. Subsequently, alternative parametrizations utilising Padé expansions ([Aviles et al. 2014](#)), Chebyshev polynomials ([Capozziello et al. 2018](#)), and logarithmic polynomials ([Bargiacchi et al. 2021](#)) have been proposed. A comprehensive comparison of these methodologies was conducted in [Hu & Wang \(2022\)](#). However, given that the localized FRBs data we utilise falls within the range $0.0039 < z < 0.66$, the z -parametrization is suitable for our analysis.

It is worth emphasizing that the parameters H_0 , q_0 , j_0 , and s_0 are solely defined within the cosmographic framework and do not inherently relate to any specific cosmological content. To establish a connection between these parameters and the characteristics of a particular cosmological model, the Einstein equations, specifically the Friedmann equations, must be additionally considered. However, in this study, our objective does not involve relating the cosmographic parameters to any specific cosmological model. Instead, we focus on directly measuring the expansion through kinematic quantities and mapping its temporal evolution. Consequently, our set of free parameters is denoted as $\theta = \{H_0, \Omega_b h^2, q_0, j_0, s_0, f_{\text{IGM}}\}$.

4 METHOD

The main purpose of this study is to verify how cosmography, or cosmic kinematics, might be helpful when constraining cosmic expansion by using Fast Radio Bursts along with its redshift measurements. In this context, first, we define two models based on the assumptions taken for the distributions of DM_{IGM} and DM_{host} , in the first one we follow [Hagstotz et al. \(2022\)](#), and in the second one we follow [Macquart et al. \(2020\)](#):

- (I) For the first model, we consider gaussian distributions for both DM_{IGM} and DM_{host} and then, every observed dispersion measure DM_i at a redshift z_i will be related to a gaussian individual likelihood,

$$\mathcal{L}(\text{DM}_i, z_i) = \frac{1}{\sqrt{2\pi\sigma_i^2}} \exp \left[-\frac{(\text{DM}_i - \text{DM}_{\text{theo}}^{\text{theo}}(z_i))^2}{2\sigma_i^2} \right], \quad (19)$$

where $\text{DM}_{\text{theo}}^{\text{theo}}(z_i)$ is the theoretical contribution as stated in section 2,

$$\begin{aligned} \text{DM}_{\text{theo}}^{\text{theo}}(z_i) &= \text{DM}_{\text{obs}} - \text{DM}_{\text{ISM}} - \text{DM}_{\text{halo}} \\ &= \text{DM}_{\text{IGM}}(z_i) + \text{DM}_{\text{host}}(z_i). \end{aligned} \quad (20)$$

The effect of measurement errors on DM_{IGM} is minimal, and as a result, the overall variation is determined by the individual uncertainties which encompass the spread from the intergalactic medium contribution, the Milky Way electron distribution

model, and the host galaxy:

$$\sigma^2(z_i) = \sigma_{\text{MW}}^2 + \sigma_{\text{host}}^2(z_i) + \sigma_{\text{IGM}}^2(z_i). \quad (21)$$

Given that all events are independent, the combined likelihood of the sample is simply the multiplication of the separate likelihoods:

$$\mathcal{L}_{\text{tot}} = \prod_i \mathcal{L}_i, \quad (22)$$

and the computation of the product is executed for every FRB listed in Table 1.

- (II) For the second model, we consider that the distribution of DM_{IGM} is quasi-gaussian distributed according to eq. (8), and for the DM_{host} we assume the lognormal distribution given by eq. (11). The total probability density function of a FRB being detected at a redshift z_i with $\text{DM}_{\text{theo}}^{\text{theo}}(z_i)$ given by eq. (20) is determined by the following relation:

$$\begin{aligned} P_i(\text{DM}_{\text{theo}}^{\text{theo}}(z_i)) &= \int_0^{\text{DM}_{\text{theo}}^{\text{theo}}} P_{\text{host}}(\text{DM}_{\text{host}}) \\ &\times P_{\text{IGM}}(\text{DM}_{\text{IGM}}) d\text{DM}_{\text{host}}, \end{aligned} \quad (23)$$

with $P_{\text{host}}(\text{DM}_{\text{host}})$ and $P_{\text{IGM}}(\text{DM}_{\text{IGM}})$ being the probability density functions for DM_{host} and DM_{IGM} as described in section 3. Finally, we calculate the joint likelihood function by combining the probability density functions of each FRB through the product:

$$\mathcal{L}_{\text{tot}} = \prod_i P_i(\text{DM}_{\text{theo}}^{\text{theo}}(z_i)). \quad (24)$$

In this study, we used the Nested Sampling algorithm – via the publicly available Python package [PolyChord](#) ([Handley et al. 2015](#)), which is a Monte Carlo (MC) technique, to place constraints on H_0 , $\Omega_b h^2$, q_0 , j_0 , s_0 and f_{IGM} parameters. We have implemented these methods to a sample of 23 localised FRBs using the two models described above (I and II) in order to estimate the set of best-fit parameters for each model. Nested sampling is a powerful method for Bayesian parameter estimation because it has several advantages over other methods, such as Markov Chain Monte Carlo (MCMC). It enables us to extensively explore the parameter space and to accurately determine the probability distributions of the parameters of interest. It also provides a way to compute the evidence of a model, i.e., the probability of the data given a model, which is important for model comparison and selection. Furthermore, certain calculations presented in this paper were made feasible by modifying the publicly available Python code, FRB ([Prochaska et al. 2019a](#)).

5 DATA AND RESULTS

5.1 Localized Fast Radio Bursts

To date, numerous Fast Radio Bursts (FRBs) have been documented by various collaborations, with a total count surpassing 1000. However, a relatively small fraction of these FRBs, specifically 24, have measurements of their redshift available. In our analysis, we focus on a subset of these FRBs, compiled by [Yang et al. \(2022\)](#), precisely the 23 instances listed in Table 1, which includes both their redshift and observed dispersion measure (DM) values. It is worth mentioning that some of these FRBs exhibit a repeating behavior. This characteristic enables the possibility of detecting their source through interferometry techniques ([Chatterjee et al. 2017](#)). The first

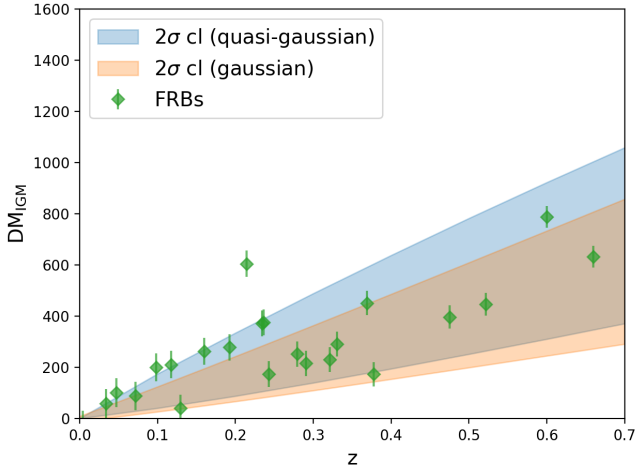


Figure 1. The 2σ confidence level region for the two distribution models considered in this work plotted as shaded areas. The blueish represents the quasi-gaussian distribution as described by Eq. (8) and the orangish represents the gaussian one. The well-localised FRBs are plotted as scatters.

Table 1. Properties of localised FRBs.

Name	Redshift	DM_{obs} (pc cm^{-3})	Reference
FRB 121102	0.19273	557	Spitler et al. (2016)
FRB 180301	0.3304	534	Bhandari et al. (2022)
FRB 180916	0.0337	348.8	Marcote et al. (2020)
FRB 180924	0.3214	361.42	Bannister et al. (2019)
FRB 181030	0.0039	103.5	Bhardwaj et al. (2021b)
FRB 181112	0.4755	589.27	Prochaska et al. (2019b)
FRB 190102	0.291	363.6	Bhandari et al. (2020)
FRB 190523	0.66	760.8	Ravi et al. (2019)
FRB 190608	0.1178	338.7	Chittidi et al. (2021)
FRB 190611	0.378	321.4	Day et al. (2020)
FRB 190614	0.6	959.2	Law et al. (2020)
FRB 190711	0.522	593.1	Heintz et al. (2020)
FRB 190714	0.2365	504.13	Heintz et al. (2020)
FRB 191001	0.234	506.9	Heintz et al. (2020)
FRB 191228	0.2432	297.5	Bhandari et al. (2022)
FRB 200430	0.16	380.25	Heintz et al. (2020)
FRB 200906	0.3688	577.8	Bhandari et al. (2022)
FRB 201124	0.098	413.52	Fong et al. (2021)
FRB 210117	0.2145	730.0	James et al. (2022)
FRB 210320	0.2797	384.8	James et al. (2022)
FRB 210807	0.12927	251.9	James et al. (2022)
FRB 211127	0.0469	234.83	James et al. (2022)
FRB 211212	0.0715	206.0	James et al. (2022)

documented repeating FRB, named FRB 121102, was originally identified by observations made using the Arecibo radio telescope (Spitler et al. 2016). Since then, numerous subsequent pulses have been detected from this particular source, with a previous study noting a period of activity lasting for approximately 157 days (Rajwade et al. 2020). Notably, among the localized FRBs, a subset of 7 FRBs has been reported to exhibit repeating behavior. In our analysis we chose to exclude the nearest point: FRB200110E as it carries little cosmological information. This is the closest extra-galactic FRB de-

tected so far, located in the M81 galaxy, only 3.6 Mpc distant from Earth (Bhardwaj et al. 2021a; Kirsten et al. 2021).

To start the analysis, first, we have to estimate DM_{IGM} for the two models considered here. The estimated DM_{IGM} of the localised FRBs are displayed in Fig. 1 as scatters along with their error bars calculated using the eq. (7). The greenish-shaded area refers to the 95% confidence region for the scatter around the mean intergalactic medium DM component considering the dispersion from eq.(8), and the yellowish-shaded represents the gaussian distribution as described in section 2. In both cases, FRB 210117 is off the 95% region, which is possibly caused by its local environment contribution to the dispersion measure (Yang et al. 2022). We chose to keep this data point in our calculations despite this outlier feature because we did not detect any relevant difference with our final results by retiring this point.

To ensure the independent and accurate determination of the parameters in Eq. (18), it is essential to constrain H_0 , $\Omega_b h^2$, and f_{IGM} as independently as possible. Here we have explored two distinct scenarios: a) In the first case, we have imposed a narrow prior on $\Omega_b h^2$, consistent with observations from primordial nucleosynthesis (BBN) and the cosmic microwave background (CMB). We have fixed the value of f_{IGM} and treated H_0 as a free parameter. The primary objective of this analysis is to derive information about H_0 , q_0 , j_0 , and s_0 . b) In the second case, we have imposed a narrow prior on both $\Omega_b h^2$ and H_0 , while allowing f_{IGM} to be a free parameter. Here, our focus is on obtaining insights into f_{IGM} , q_0 , j_0 , and s_0 . In both cases a) and b) we use the the following flat priors: $[-0.95, -0.3]$ for q_0 , $[0, 2]$ for j_0 and $[-5, -10]$ for s_0 .

In case a), two types of priors were considered for $\Omega_b h^2$, taking into account consistency with Big Bang nucleosynthesis (BBN) and the cosmic microwave background (CMB). The first prior is a flat prior within the interval $[0.02186, 0.02284]$, which aligns with findings from previous studies (Aghanim et al. 2020; Cooke et al. 2018). The second prior is a Gaussian prior with $\Omega_b h^2 = 0.02235 \pm 0.00049$, in agreement with the value reported by Cooke et al. (2018). Additionally, a flat prior on H_0 within the range $[50, 80]$ was applied, and the value of f_{IGM} was fixed at 0.82, as estimated by Shull et al. (2012). The results for this case are presented in Table 2 and Fig. 2 for both Models I and II.

Table 2. The constraints for the cosmographic parameters of the DM – z relation when considering different priors over $\Omega_b h^2$. The results for H_0 are displayed with 6% and 7% precision.

Prior on $\Omega_b h^2$	Model	H_0	q_0	j_0	s_0
Gaussian	I	$69.5^{+3.6}_{-4.0}$	-0.63 ± 0.18	$0.64^{+0.36}_{-0.50}$	-4.0 ± 6.3
	II	69.4 ± 4.7	$-0.59^{+0.20}_{-0.17}$	$1.08^{+0.62}_{-0.56}$	-2.1 ± 7.0
Flat	I	70.0 ± 3.9	-0.61 ± 0.19	$0.72^{+0.39}_{-0.51}$	$-4.6^{+6.8}_{-6.0}$
	II	70.0 ± 5.3	-0.60 ± 0.19	$1.10^{+0.66}_{-0.55}$	-2.4 ± 7.1

The determined values of H_0 can be observed in Table 2: $H_0 = 69.5^{+3.6}_{-4.0}$ $\text{km s}^{-1} \text{Mpc}^{-1}$ and $H_0 = 69.4^{+5.4}_{-4.8}$ $\text{km s}^{-1} \text{Mpc}^{-1}$ for the Gaussian $\Omega_b h^2$ prior, and $H_0 = 70.0 \pm 3.9$ $\text{km s}^{-1} \text{Mpc}^{-1}$ and $H_0 = 70.0 \pm 5.3$ $\text{km s}^{-1} \text{Mpc}^{-1}$ for the flat prior case. All four values exhibit good agreement within the 1σ statistical confidence level, both among themselves and with previous results reported, such as those derived from Supernovas type Ia (Riess et al. 2022), Cosmic Chronometers (Gómez-Valent & Amendola 2018), and recent FRB-based investigations within the Λ CDM framework (Wu et al. 2022;

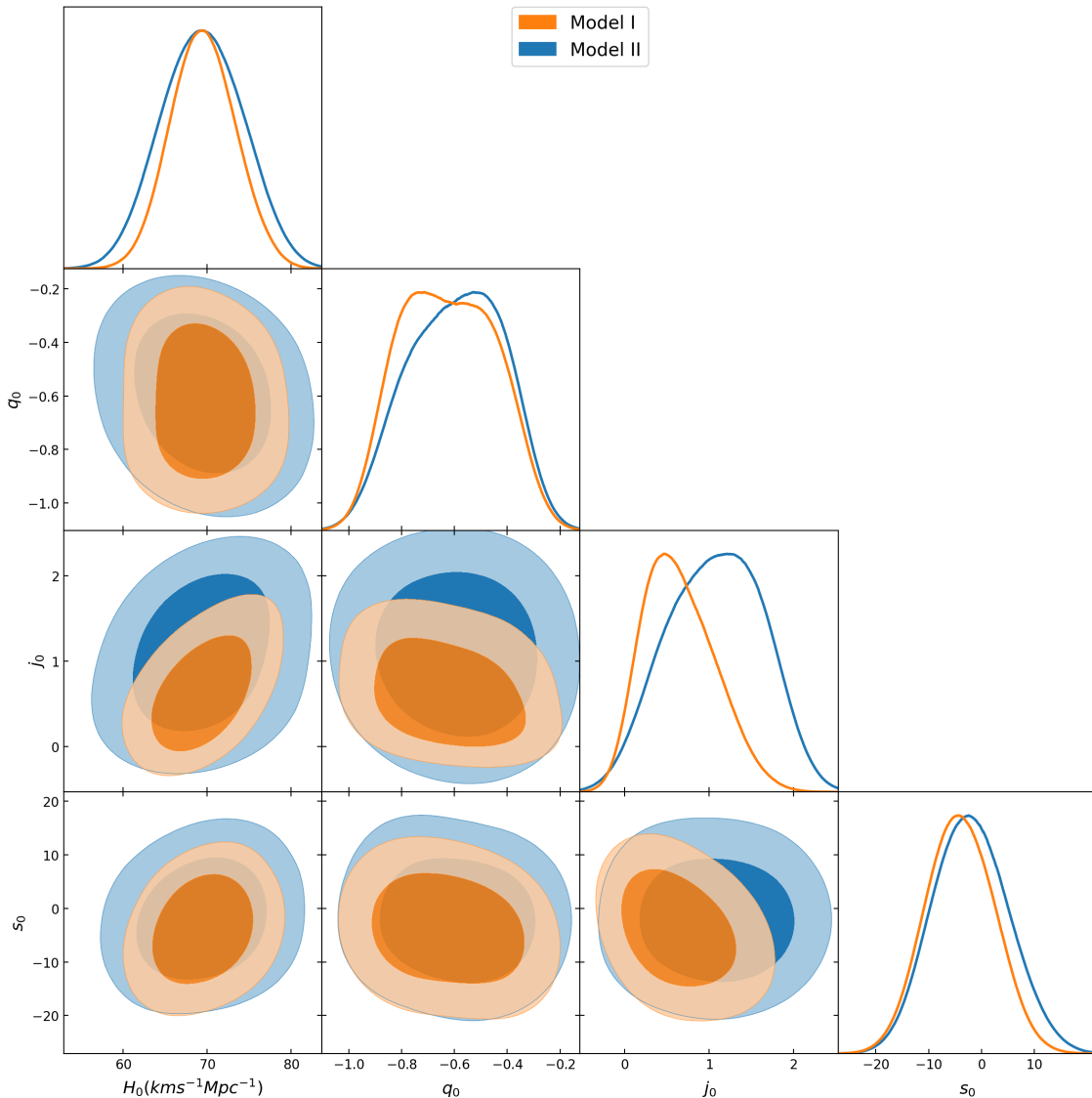


Figure 2. Comparison between the constraints for the two models considered in this work using the 23 well-localised FRBs sample when fixing f_{IGM} and considering a gaussian prior on $\Omega_b h^2$.

Zhao et al. 2022). Nevertheless, the large error bars associated with these values limit their informativeness regarding the Hubble tension. In terms of precision, the use of the 23 FRB data points allows for a H_0 precision of approximately $\sim 6\%$ for Model I and $\sim 7\%$ for Model II.

The results for the deceleration parameter q_0 presented in Table 2 exhibit agreement within a 1σ confidence level, indicating an accelerated expansion. In fact, a decelerated phase is rejected at a significance level of approximately 3.2σ , corresponding to a probability of approximately 99.97%. These findings are particularly interesting as they are derived solely from the analysis of FRBs data. However, it is important to note that the error bars for q_0 are relatively large. While our results suggest a precision of around 32% for this parameter, it decreases significantly when considered in conjunction with other observational probes (see below). Similar to q_0 , the jerk parameter j_0 also demonstrates agreement within a 1σ confidence level for all values reported in Table 2. Notably, the Λ CDM value of $j_0 = 1$ lies within the 1σ interval for all cases, although the error bar

for this parameter is roughly of the same magnitude as that of q_0 . Note that there is a slight discrepancy between the mean values for j_0 in both models. In contrast, the snap parameter s_0 exhibits poor constraint from the FRBs data. While all estimated values for s_0 in our analysis are in agreement at 1σ C.L. between each other and the Λ CDM snap s_0 value is inside of such interval, it is not possible to discern whether the Universe possesses an evolving dark energy component or a constant one. Consequently, in general, further data and analysis are needed to refine our understanding and provide more precise constraints on the values of H_0 , q_0 , j_0 , and s_0 .

The contour plots corresponding to the results presented in Table 2 are displayed in Fig. 2. The findings for both models I and II exhibit striking similarity, with only slight discrepancies observed in the H_0 - j_0 , j_0 - q_0 , and j_0 - s_0 planes. It is worth noting that, similar to other probes such as supernovae type Ia (SNIa) and cosmic chronometers (CC), the q_0 - H_0 plane derived from FRBs data showcases an anticorrelation trend. Additionally, the j_0 - q_0 plane exhibits some extremely weak correlation features and interestingly the j_0 - H_0 plane exhibits

a positive correlation different than anticorrelation in SNIa and CC case. These patterns suggest that tests employing FRBs data could arise as complementary to other probes at the background level. We will delve further into this point in the subsequent discussion.

Table 3. The constraints for the cosmographic expansion up to the snap parameter. In this case, we assume a gaussian prior to $\Omega_b h^2$ and a narrow prior over H_0 .

Model	q_0	j_0	s_0	f_{IGM}
I	-0.61 ± 0.19	$0.67^{+0.37}_{-0.50}$	-4.6 ± 6.6	0.84 ± 0.06
II	$-0.59^{+0.23}_{-0.16}$	1.02 ± 0.56	-1.7 ± 6.7	0.82 ± 0.07

On the other hand, in case b), we consider a Gaussian prior for $\Omega_b h^2$ with a value of 0.02235 ± 0.00049 , as reported by [Cooke et al. \(2018\)](#). Additionally, we impose a narrow flat prior on H_0 within the range [66, 75], in line with the framework addressing the Hubble tension. This choice allows us to estimate the baryon fraction in the intergalactic medium f_{IGM} , alongside q_0 , j_0 , and s_0 . The results for this case are summarized in Table 3. Regarding f_{IGM} , both models I and II agree within a 1σ confidence level, as well as with previous studies. The analysis suggests that approximately 82% of the baryons are accounted for in the late-time Universe, consistent with the findings of [Shull et al. \(2012\)](#). The precision of this result is approximately 7% for model I and 8% for model II. In terms of q_0 and j_0 , the results are consistent in both models. Despite the high uncertainties, all the results remain consistent with each other. Our results are in accordance with those in [Shull et al. \(2012\)](#). Their analysis suggests that approximately 18 \pm 4% of the baryons in the Universe are in a collapsed form, with 7 \pm 2% residing in galaxies, 4 \pm 1.5% in the intercluster medium (ICM), 5 \pm 3% in the circumgalactic medium (CGM), and 1.7 \pm 0.4% in cold neutral gas clouds, estimating that roughly 100% of the baryons are found in low redshift.

Considering the limited constraints and theoretical motivations for DM_{host} , we also explored scenarios where the mean values of the distributions for this component, denoted as $(\text{DM}_{\text{host}})$ and e^μ in models I and II respectively, are treated as free parameters. Our investigation reveals that incorporating it them as a fixed value, weighted by the redshift of the source, yields comparable results without significant differences.

5.2 Combined constraints with CC, SNIa, and FRBs

To compare our results with other results in the literature, we use 27 of the 41 measurements of the Hubble parameter $H(z)$ compiled by [Jesus et al. \(2018\)](#), inferred through the cosmic chronometers technique and also using the position of the peak of Baryon Acoustic Oscillations, which provides a standard rule in the radial direction when measuring the distribution of galaxies by mapping the large scale structure. The approach presented in [Jimenez & Loeb \(2002\)](#) relies on measuring the age difference Δt between pairs of old spiral galaxies that formed at comparable times but are separated by a distance Δz . This method is particularly suitable for galaxies with low levels of stellar dust, such as the selected spiral galaxies, which allows for easier acquisition of their luminous spectra ([Padilla et al. 2021](#)). By applying this technique, researchers can estimate the Hubble parameter using the following relationship:

$$H(z) = -\frac{1}{1+z} \frac{dz}{dt} \approx -\frac{1}{1+z} \frac{\Delta z}{\Delta t}. \quad (25)$$

By observing galaxies at remote times, we can use the age evolution of their stars as a clock to measure cosmic time. This method has a significant advantage as it avoids systematic errors that may arise when measuring the absolute ages of individual galaxies, instead allowing for the measurement of the relative age difference (dt) between them. Additionally, this approach enables the independent inference of the Hubble parameter, without relying on a specific cosmological model, as pointed out by [Negrelli et al. \(2020\)](#). To estimate the cosmographic parameters from Cosmic Chronometers, we need to evaluate the likelihood function, computed as follows:

$$\mathcal{L}_{\text{CC}} \propto \exp \left[-\frac{(H_i - H^{\text{theo}}(z_i))^2}{2\sigma_{H_i}^2} \right], \quad (26)$$

where H_i represents each of the individual measurements of the sample considered and H^{theo} , are the set of Hubble parameters calculated from the cosmographic expansion, see [Lizardo et al. \(2021\)](#).

We also include supernovae type Ia (SNIa) in our analysis, covering the same redshift range as the FRBs in Table 1. Specifically, we construct a subsample of the Pantheon catalogue, which consists of 926 data points. The Pantheon dataset comprises a comprehensive collection of SNIa observations, incorporating data from various surveys such as PanSTARRS1, SDSS, SNLS, and various low- z and HST samples ([Scolnic et al. 2018](#)). The redshift range of the SNIa data spans from 0.01 to 2.26. The distance modulus for SNIa is defined as follows:

$$\mu_{\text{obs}} = m_{\text{B}} - M_{\text{B}}, \quad (27)$$

being m_{B} the apparent magnitude and M_{B} the absolute magnitude. Using the luminosity distance relation,

$$d_{\text{L}} = (1+z) \frac{c}{H_0} \int_0^z \frac{dz'}{E(z')}, \quad (28)$$

the theoretical distance modulus is expressed as:

$$\mu_{\text{th}} = 5 \log_{10} \left(\frac{d_{\text{L}}}{\text{Mpc}} \right) + 25. \quad (29)$$

By fitting this quantity, it is possible to obtain constraints from SNIa through the relation:

$$\mathcal{L}_{\text{SNIa}} \propto \exp \left[-\frac{1}{2} (\mu_{\text{obs}} - \mu_{\text{th}})^T \mathbf{C}^{-1} (\mu_{\text{obs}} - \mu_{\text{th}}) \right], \quad (30)$$

where μ_{obs} are the observed distance modulus and \mathbf{C} is the covariance matrix of the events, check [Scolnic et al. \(2018\)](#) for more information.

Considering that model II has more theoretical motivations and simulations support it, we have chosen this model for the joint analysis. Nevertheless, it is important to note that even working with model II, the limited number of FRB data and the striking similarity between models I and II results (see Table 2), suggest that there is no huge difference in working with any of them. To perform the joint analysis, we combine the FRB dataset with Cosmic Chronometers and type Ia Supernovae. In this case, the free parameters are $\theta = \{H_0, \Omega_b h^2, q_0, j_0, s_0, M_{\text{B}}\}$, with a Gaussian prior over M_{B} , with a mean value of -19.24 , and a standard deviation of 0.04 given by [Camarena & Marra \(2021\)](#). The total likelihood then is the product:

$$\mathcal{L}_{\text{TOT}} = \mathcal{L}_{\text{FRB}} \times \mathcal{L}_{\text{CC}} \times \mathcal{L}_{\text{SNIa}}. \quad (31)$$

The statistical results are summarized in Table 4 and displayed in

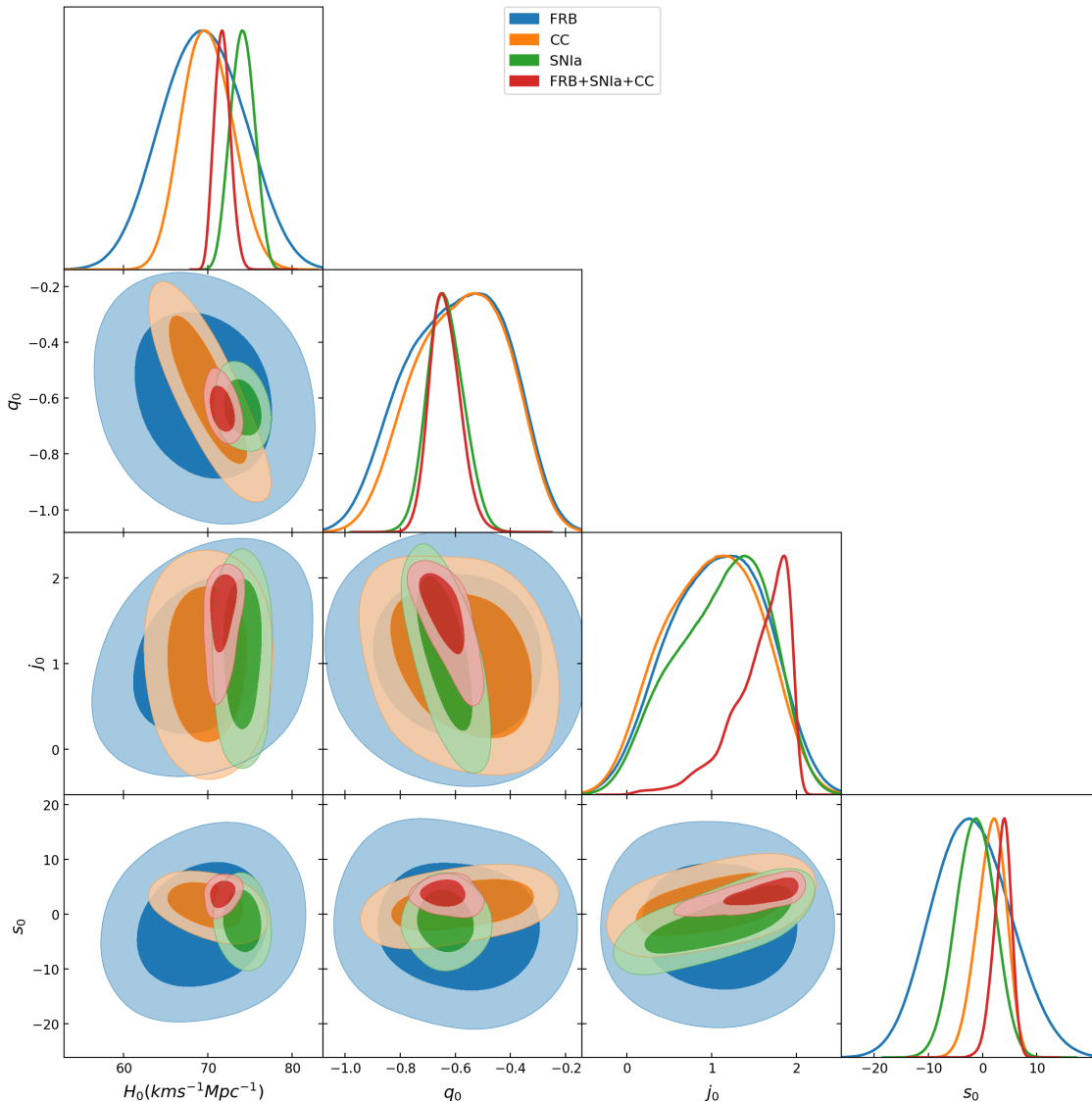


Figure 3. The posterior distribution with the 1σ and 2σ statistical confidence regions for the parameters H_0 , q_0 , j_0 , and s_0 , constrained by FRBs, CC, SNIa.

Fig. 3. Our combined constraint for Hubble constant H_0 achieves a precision of $\sim 1\%$. It is worth noting a preference for lower values of H_0 when utilising Cosmic Chronometers. This preference holds whether employing the cosmography technique or working within the framework of the Λ CDM model (Moresco et al. 2022; Busti et al. 2014) and, as a result, a subtle tension of $\sim 1.2\sigma$ arises in comparison to the constraints obtained from type Ia Supernovae, causing such a small precision in the joint constraint. The deceleration parameter q_0 achieves a precision of $\sim 9\%$ while the jerk j_0 has a precision of $\sim 26\%$. Furthermore, it is worth mentioning that although the snap parameter s_0 does not align within the 1σ region of the Λ CDM model, the inclusion of FRBs in conjunction with Cosmic Chronometers and type Ia Supernovae reduces the error associated with this parameter by approximately 30%.

6 DISCUSSION

Fast Radio Bursts (FRBs) have become an increasingly valuable tool in cosmological research, with the DM – z relation being employed

Table 4. Constraints for all the parameters using the model I with a gaussian prior on $\Omega_b h^2$ and fixing $f_{\text{IGM}} = 0.82$.

Parameter	FRB	CC	SNIa	FRB+CC+SNIa
H_0	69.4 ± 4.7	69.9 ± 2.9	74.1 ± 1.4	$71.6^{+0.9}_{-1.0}$
q_0	$-0.59^{+0.20}_{-0.17}$	-0.57 ± 0.16	$-0.64^{+0.05}_{-0.07}$	$-0.64^{+0.05}_{-0.06}$
j_0	$1.08^{+0.62}_{-0.56}$	1.01 ± 0.55	$1.13^{+0.66}_{-0.47}$	$1.57^{+0.42}_{-0.15}$
s_0	-2.1 ± 7.0	$1.6^{+2.9}_{-2.4}$	-1.3 ± 3.5	$3.6^{+1.8}_{-1.4}$

in numerous previous studies. In this work, we expand upon this analysis by introducing the cosmographic expansion of the DM – z expression. To assess the reliability of our approach, we consider two distinct models. The first model incorporates straightforward assumptions and treats the host and intergalactic medium (IGM) components as Gaussian distributions. The second model is more intricate, assuming a quasi-Gaussian distribution for the IGM component and a lognormal distribution for the host component. Our results indicate that both approaches yield significant improvements

over previous studies that solely relied on the $DM-z$ relation, achieving an interesting precision of 6% for model I and 7% for model II for the Hubble parameter (H_0) despite the limited number of measured FRBs. According to the standard error formula, we estimate that approximately 2400 FRBs with redshift measurements are required to achieve a similar precision level as the SH0ES collaboration. Fortunately, this goal is within reach in the near future, given the growing number of instruments dedicated to the detection of FRBs. Two prominent upcoming radio telescopes deserve mention: the Square Kilometre Array (SKA) and the Baryon Acoustic Oscillations from Integrated Neutral Gas Observations (BINGO) project. The SKA, renowned for its sub-arcsecond accuracy (Zhang et al. 2023), promises to revolutionize FRB (Fast Radio Burst) research by enabling the detection of thousands of FRBs and their redshift counterparts (Macquart et al. 2015). On the other hand, the BINGO project, currently under construction in Brazil (Abdalla et al. 2022; Santos et al. 2023), focuses specifically on detecting the 21-cm line of neutral hydrogen (HI) and is also expected to be a formidable instrument for FRB detection.

By employing the cosmographic expansion, we successfully estimated the kinematic parameters q_0 , j_0 , and s_0 for both models. Notably, our findings exhibited strong agreement between the two models I and II, but it must be recalled that model II has more theoretical foundations and support from cosmological simulations. Utilising only FRBs, we obtained compelling evidence for the acceleration of the expanding Universe. Moreover, the results from both models indicated the presence of a transitional phase during which the dynamics of the universe underwent a change. However, given the limited constraints on the snap parameter, further data are required to discern whether the accelerated expansion is governed by a constant dark energy component or a time-evolving one.

In addition, the present study has investigated how the cosmographic expansion up to the snap parameter can impact on the estimation of the fraction of baryons in the intergalactic medium (IGM). Our analysis revealed that all the models we considered yielded very consistent results that were in agreement with previous studies. Despite the large statistical errors, we were able to address the missing baryon problem by utilising well-localised FRBs. Our calculations yielded an estimated fraction of baryons in the IGM of $f_{\text{IGM}} = 0.82 \pm 0.06$, which suggests that the majority of baryons are indeed accounted for in the IGM. This finding is significant because it provides further insight into the distribution of matter in the universe in a model-independent way and could have implications for our understanding of cosmic structure formation.

Based on the results of this study, it is clear that cosmography has played a crucial role in advancing our understanding of FRBs and their usefulness as a cosmological tool. By incorporating higher-order kinematic parameters, such as the snap parameter, we were able to improve the precision of our estimates for the Hubble parameter and the fraction of baryons in the IGM. The high level of consistency between our models and previous studies underscores the reliability of cosmography as a technique for understanding the properties of the universe. Additionally, the continued search for new FRBs and the development of more advanced observational techniques could lead to even more precise estimates of cosmological parameters, further refining our understanding of the evolution of the Universe and its fundamental properties.

ACKNOWLEDGEMENTS

JASF thanks FAPES for financial support. WSHR thanks FAPES (PRONEM No 503/2020) for the financial support under which this work was carried out. The authors thank V. Marra for his insightful comments on this paper.

DATA AVAILABILITY

The data used in this work is publicly available at <https://www.wis-tns.org/> and <http://frbhosts.org/#explore>.

REFERENCES

- Abdalla E., et al., 2022, *Astronomy & Astrophysics*, 664, A14
 Aghanim N., et al., 2020, *Astronomy & Astrophysics*, 641, A6
 Akahori T., Ryu D., Gaensler B. M., 2016, *ApJ*, 824, 105
 Aviles A., Gruber C., Luongo O., Quevedo H., 2012, *Physical Review D*, 86, 123516
 Aviles A., Bravetti A., Capozziello S., Luongo O., 2014, *Phys. Rev. D*, 90, 043531
 Bannister K. W., et al., 2019, *Science*, 365, 565
 Bargiacchi G., Risaliti G., Benetti M., Capozziello S., Lusso E., Saccardi A., Signorini M., 2021, *A&A*, 649, A65
 Bhandari S., Flynn C., 2021, *Universe*, 7, 85
 Bhandari S., et al., 2020, *The Astrophysical Journal Letters*, 895, L37
 Bhandari S., et al., 2022, *The Astronomical Journal*, 163, 69
 Bhardwaj M., et al., 2021a, *The Astrophysical Journal Letters*, 910, L18
 Bhardwaj M., et al., 2021b, *The Astrophysical Journal Letters*, 919, L24
 Bochenek C. D., Ravi V., Belov K. V., Hallinan G., Kocz J., Kulkarni S. R., McKenna D. L., 2020, *Nature*, 587, 59
 Busti V. C., Clarkson C., Seikel M., 2014, *Monthly Notices of the Royal Astronomical Society: Letters*, 441, L11
 Camarena D., Marra V., 2021, *Monthly Notices of the Royal Astronomical Society*, 504, 5164
 Capozziello S., D’Agostino R., Luongo O., 2018, *MNRAS*, 476, 3924
 Cattoën C., Visser M., 2007, *Classical and Quantum Gravity*, 24, 5985
 Chatterjee S., et al., 2017, *Nature*, 541, 58
 Chittidi J. S., et al., 2021, *The Astrophysical Journal*, 922, 173
 Cooke R. J., Pettini M., Steidel C. C., 2018, *The Astrophysical Journal*, 855, 102
 Cordes J. M., Lazio T. J. W., 2002, arXiv preprint astro-ph/0207156
 Day C. K., et al., 2020, *Monthly Notices of the Royal Astronomical Society*, 497, 3335
 Deng W., Zhang B., 2014, *The Astrophysical Journal Letters*, 783, L35
 Fong W.-f., et al., 2021, *The Astrophysical Journal Letters*, 919, L23
 Fukugita M., Hogan C., Peebles P., 1998, *The Astrophysical Journal*, 503, 518
 Gao H., Li Z., Zhang B., 2014, *ApJ*, 788, 189
 Gómez-Valent A., Amendola L., 2018, *Journal of Cosmology and Astroparticle Physics*, 2018, 051
 Hagstotz S., Reischke R., Lilow R., 2022, *Monthly Notices of the Royal Astronomical Society*, 511, 662
 Handley W., Hobson M., Lasenby A., 2015, *Monthly Notices of the Royal Astronomical Society: Letters*, 450, L61
 Heinesen A., 2021, *Phys. Rev. D*, 104, 123527
 Heintz K. E., et al., 2020, *The Astrophysical Journal*, 903, 152
 Hu J. P., Wang F. Y., 2022, *A&A*, 661, A71
 Jalilvand F., Mehrabi A., 2022, *The European Physical Journal Plus*, 137, 1341
 James C., et al., 2022, *Monthly Notices of the Royal Astronomical Society*, 516, 4862
 Jaroszynski M., 2019, *Monthly Notices of the Royal Astronomical Society*, 484, 1637
 Jesus J., Gregório T. M., Andrade-Oliveira F., Valentim R., Matos C. A., 2018, *Monthly Notices of the Royal Astronomical Society*, 477, 2867

- Jimenez R., Loeb A., 2002, *The Astrophysical Journal*, 573, 37
- Kirsten F., et al., 2021, arXiv preprint arXiv:2105.11445
- Law C. J., et al., 2020, *The Astrophysical Journal*, 899, 161
- Lazkoz R., Alcaniz J., Escamilla-Rivera C., Salzano V., Sendra I., 2013, *Journal of Cosmology and Astroparticle Physics*, 2013, 005
- Lemos T., Gonçalves R. S., Carvalho J. C., Alcaniz J. S., 2022, arXiv preprint arXiv:2205.07926
- Li Z., Gao H., Wei J.-J., Yang Y.-P., Zhang B., Zhu Z.-H., 2020, *Monthly Notices of the Royal Astronomical Society: Letters*, 496, L28
- Lin H.-N., Tang L., Zou R., 2023, *MNRAS*, 520, 1324
- Lizardo A., Amante M. H., García-Aspeitia M. A., Magaña J., Motta V., 2021, *Monthly Notices of the Royal Astronomical Society*, 507, 5720
- Lobo F. S. N., Mimoso J. P., Visser M., 2020, *J. Cosmology Astropart. Phys.*, 2020, 043
- Lorimer D. R., Bailes M., McLaughlin M. A., Narkevic D. J., Crawford F., 2007, *Science*, 318, 777
- Macquart J.-P., et al., 2015, arXiv preprint arXiv:1501.07535
- Macquart J.-P., et al., 2020, *Nature*, 581, 391
- Marcote B., et al., 2020, *Nature*, 577, 190
- McQuinn M., 2013, *The Astrophysical Journal Letters*, 780, L33
- McQuinn M., 2014, *ApJ*, 780, L33
- Moresco M., et al., 2022, *Living Reviews in Relativity*, 25, 6
- Negrelli C., Kraisselburd L., Landau S., Scóccola C. G., 2020, *Journal of Cosmology and Astroparticle Physics*, 2020, 015
- Nusser A., 2016, *ApJ*, 821, L2
- Ocker S. K., Cordes J. M., Chatterjee S., 2021, *ApJ*, 911, 102
- Padilla L. E., Tellez L. O., Escamilla L. A., Vazquez J. A., 2021, *Universe*, 7, 213
- Petroff E., Hessels J., Lorimer D., 2019, *The Astronomy and Astrophysics Review*, 27, 1
- Pourojaghi S., Zabihi N. F., Malekjani M., 2022, *Phys. Rev. D*, 106, 123523
- Prochaska J. X., Zheng Y., 2019, *Monthly Notices of the Royal Astronomical Society*, 485, 648
- Prochaska J. X., Simha S., Law C., Tejos N., et al., 2019a, Zenodo
- Prochaska J. X., et al., 2019b, *Science*, 366, 231
- Rajwade K., et al., 2020, *Monthly Notices of the Royal Astronomical Society*, 495, 3551
- Ravi V., et al., 2019, *Nature*, 572, 352
- Riess A. G., et al., 2022, *The Astrophysical Journal Letters*, 934, L7
- Rocha B. A. R., Martins C. J. A. P., 2023, *MNRAS*, 518, 2853
- Santos M. V. d., et al., 2023, arXiv preprint arXiv:2308.06805
- Scolnic D. M., et al., 2018, *The Astrophysical Journal*, 859, 101
- Shao L., Zhang B., 2017, *Phys. Rev. D*, 95, 123010
- Shull J. M., Smith B. D., Danforth C. W., 2012, *The Astrophysical Journal*, 759, 23
- Spitler L., et al., 2016, *Nature*, 531, 202
- Tingay S. J., Kaplan D. L., 2016, *ApJ*, 820, L31
- Visser M., 2005, *General Relativity and Gravitation*, 37, 1541
- Wei J.-J., Gao H., Wu X.-F., Mészáros P., 2015, *Phys. Rev. Lett.*, 115, 261101
- Weinberg S., 1972, *Gravitation and cosmology: principles and applications of the general theory of relativity*
- Wu X.-F., et al., 2016, *ApJ*, 822, L15
- Wu Q., Yu H., Wang F., 2020, *The Astrophysical Journal*, 895, 33
- Wu Q., Zhang G.-Q., Wang F.-Y., 2022, *Monthly Notices of the Royal Astronomical Society: Letters*, 515, L1
- Yang K., Wu Q., Wang F., 2022, *The Astrophysical Journal Letters*, 940, L29
- Yao J., Manchester R., Wang N., 2017, *The Astrophysical Journal*, 835, 29
- Zhang B., 2020, *Nature*, 587, 45
- Zhang J.-G., Zhao Z.-W., Li Y., Zhang J.-F., Li D., Zhang X., 2023, arXiv preprint arXiv:2307.01605
- Zhao Z.-W., Zhang J.-G., Li Y., Zou J.-M., Zhang J.-F., Zhang X., 2022, arXiv preprint arXiv:2212.13433
- Zhou B., Li X., Wang T., Fan Y.-Z., Wei D.-M., 2014, *Phys. Rev. D*, 89, 107303
- Zhou D., et al., 2022, *Research in Astronomy and Astrophysics*, 22, 124001

This paper has been typeset from a $\text{\TeX}/\text{\LaTeX}$ file prepared by the author.